A methodology to derive scour fragility functions for masonry arch bridges

G. Degan Di Dieco & M. Pregnolato

Department of Civil Engineering, University of Bristol, Bristol, UK

A.R. Barbosa

School of Civil and Construction Engineering, Oregon State University, Corvallis, USA

ABSTRACT: Frequency and intensity of hydrological hazards have increased. Consequently, riverine bridges are suffering damage due to flooding. Fragility functions are used to estimate such damage conditioned on hazard intensity. However, flood fragility functions are limited for riverine bridges, and generally lack for masonry bridges. This paper presents a methodology to derive flood fragility functions for masonry arch bridges accounting for component failure modes. Demand and capacity of bridge components are derived from existing analytical expressions, and account for aleatory uncertainties via Monte Carlo simulations. The methodology is illustrated using a UK masonry bridge, which collapsed due to winter flood-induced scour. The investigated bridge is divided into its components (e.g., arches, pier) and a scour fragility function is derived for the arch, based on a lognormal cumulative distribution fitting to the derived failure probability data. Future research will develop scour fragility functions for other bridge components.

1 INTRODUCTION

In recent years various bridges have collapsed because of increasing precipitations, floods, and lack of maintenance (Schaap and Caner, 2021). In the United Kingdom (UK), recent collapses have highlighted the vulnerability of masonry arch bridges to flooding (Solan et al., 2020). For instance, eight masonry bridges collapsed in the Cumbria region alone (Northwest of England) during the 2009 and 2015 floods, resulting in £10.49 million of reconstruction costs (Li et al., 2021). Flood-induced bridge damage can result from scour, hydrostatic or hydrodynamic actions (HE, 2020a). The literature indicates that scour is the leading cause of bridge damage (Sasidharan et al., 2021), including natural, general, contraction, and local scour (HE, 2020a).

Quantifying the flood risk of bridge portfolios is becoming crucial to reduce economical and human losses (Swiss Re, 2021). Risk is typically obtained as the product of hazard, exposure, and vulnerability (Ang and Tang, 1975). Vulnerability represents the likelihood of losses as a function of hazard intensity measure(s) (Galasso et al., 2021), where expected losses are given as the product of the expected level of damage and bridge restoration costs for the various levels of damage (Gidaris et al., 2017). The expected level of damage conditioned on hazard intensity measure(s) is referred as "fragility" and estimated via fragility functions (Wen and Ellingwood, 2005). For applying fragility functions in vulnerability assessments, structures within a portfolio are grouped in vulnerability classes (Burns et al., 2021; Mangalathu et al., 2017), i.e. groups of structures which do not have statistically significant different responses (e.g. reinforced concrete multi-column bent bridges).

Bridge flood vulnerability classes that explicitly account for bridge structural performance and their possible failure modes are currently scarce in the literature (Gidaris et al., 2017; Degan Di Dieco et al., 2022). When considering masonry arch bridges, Lamb et al. (2019) derived scour fragility functions by fitting lognormal fragility functions to probability data of historical failures, and flood return period as intensity measure. Eidsvig et al. (2021) and Mendoza Cabanzo et al. (2022) derived scour fragility functions via limit state analyses of load carrying capacity and flow discharge as intensity measure. George and Menon (2021) proposed scour fragility functions derived via

DOI: 10.1201/9781003323020-185

kinematic chain limit analyses with scour-induced pier rotation as intensity measure. Maroni et al. (2020) developed a Bayesian scour fragility function using a qualitative risk classification, scour depth data from monitoring, and relative scour depth as intensity measure. The reviewed studies show that their fragility functions do not consider failure modes of components. Subdividing a bridge into key structural components affects damage estimates of bridge portfolios (Minnucci et al., 2022; Nielson and DesRoches, 2007) and consequently their risk. As a result, the first step to build robust estimates for flood-induced damage and risk is the investigation of significant failure modes of bridge components and their interdependencies (Argyroudis and Mitoulis, 2021; Ren et al., 2019).

This paper proposes a methodology of fragility functions for masonry arch bridges which accounts for failure modes of key structural components. Figure 1 illustrates the rational of the proposed methodology for pier local scour inducing compressive rotational failure of a masonry arch; however, the methodology is derived to accommodate further components and their failure modes. In this methodology, existing analytical expressions are used to estimate bridge component capacities, while structural analysis schemes are used to estimate demands on bridge components. As a proof-of-concept, the proposed methodology is applied to a two-span masonry arch bridge which was spanning over River Calder in Halifax (West Yorkshire, North of England) and that collapsed in winter 2015 because of flood-induced scour (Tubaldi et al., 2018). This paper is divided into five sections. Section 2 details the methodology for developing fragility functions, the approach to account for scour effects on estimates of masonry arch capacity and demand, and the case study bridge. Section 3 shows the derived fragility function. Section 4 discusses underpinning assumptions and suggests future work. Section 5 summarizes the key findings.

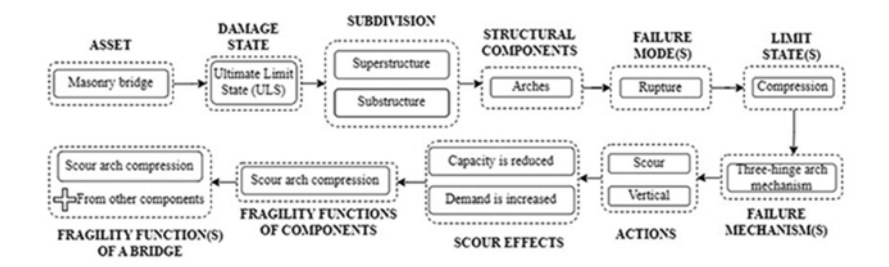


Figure 1. The proposed methodology for deriving flood fragility functions for masonry arch bridges.

2 METHODS

2.1 Fragility function derivation

Fragility functions can be derived empirically or analytically (Shinozuka et al., 2000). While empirical fragility functions are derived from observed damage data, analytical fragility functions are defined upon failure probability data, i.e. the ratio of the number of cases that exceed the failure state to the total number of simulations, for each investigated intensity measure (Mendoza Cabanzo et al., 2022). Based on structural reliability theory, the limit state function M(x) (Mendoza Cabanzo et al., 2022) is given by:

$$M(x) = R(x) - E(x) \tag{1}$$

where M(x) measures the difference between resistance effects R(x) (i.e. capacity) and load effects E(x) (i.e. demand), and x is a vector of a particular sample point. From Equation 1, it follows that failure is defined when $M(x) \le 0$. Failure data can be generated via simple Monte Carlo (MC) simulations (Schmidt et al., 2019) and fitted with a cumulative distribution function, such as the lognormal fragility function (Baker, 2015). This study focuses on the limit state function for ultimate compressive strength only.

The compressive resistance of masonry elements R (i.e. capacity) is given by Equation 4.7.1 of CD 376 (HE, 2020b):

$$R(R_c) = 0.6 \cdot F_c \cdot [R_c \cdot \mathbf{b} \cdot (t - 2e)] \tag{2}$$

where b (mm) is the element width, R_c (N/mm^2) is the basic random variable defining the masonry compressive strength, t (mm) is the overall element thickness, e (mm) is the eccentricity of the centre of compression in the element, 0.6 is a deterministic coefficient, and F_c is the condition factor and function of cracking in the arch (see Equation 6). Note that the 0.6 coefficient derives from Equation 4.7.1 in CD 376 (HE, 2020b), where $0.6 = 0.4 \gamma_M$, and $\gamma_M = 1.5$ is a partial safety factor. The masonry compressive strength R_c is assumed normally distributed with mean value \bar{r}_c and coefficient of variation CoV_c . For the normal random variable R_c , the mean value \bar{r}_c is obtained from the characteristic value f_k as follow (Melchers and Beck, 2018):

$$\bar{r}_c = f_k / (1 - k_{0.05} \cdot CoV_c)$$
 (3)

where $k_{0.05}$ is the value of the standard normal variable for a probability of 0.05, f_k is given by Equation 3.1 of BS EN 1996-1-1:2005 (BSI, 2013):

$$f_k = K f_b^{\alpha} f_m^{\beta} \tag{4}$$

where α , β , and K are constants, function of mortar and unit type, and listed at paragraph 3.6.1.2 of BS EN 1996-1-1:2005 (BSI, 2013), f_m is the mean compressive mortar strength, and f_b is the normalised mean compressive unit strength (i.e. brick), in the direction of the applied action effect, and all these variables have been considered deterministic. Annex 2 of Morton (2012) provides the equation for f_b :

$$f_b = CF \cdot \delta \cdot f_{bm} \tag{5}$$

with both CF conditioning factor and δ shape factor related to brick tests given by Annex A of BS EN 772-1:2011 (BSI, 2015), f_{bm} is the mean compressive strength of the unit, and all these variables have been considered deterministic. The condition factor F_c , given by Equations 7.5.1a,b of CS 454 (HE, 2020c), is used to consider the material degradation defects in arch conditions:

$$F_c = F_{cM}F_i = F_{cM}(F_w F_d F_{mo}) \tag{6}$$

where F_{CM} is the arch barrel condition factor, F_j is the joint factor for arch diagonal cracks, F_w is the joint width factor, F_d is the joint depth factor, and F_{mo} is the mortar factor. The value of F_{CM} and F_j shall be determined according to Tables 7.5.1a,b,c,d of CS 454 (HE, 2020c) after a bridge inspection; however, their values have been assumed in this study, and considered deterministic.

The compressive load effect E (i.e. demand) is determined according to the assessment level 1 of CS 454 (HE, 2020c), where simple structural analyses are carried out and the masonry tensile strength is neglected:

$$E(\Gamma_m) = S_a(\Gamma_m)/\Phi_i \tag{7}$$

where $S_a(\Gamma_m)$ is the compressive force in the component, linear function of the unit weight of masonry Γ_m [see Equation 45 in Chapter 3 of Como (2013)], and Φ_i is the slenderness and eccentricity factor given by Equation 6.4 of BS EN 1996-1-1:2005 (BSI, 2013). Note that the compressive force in the component $S_a(\Gamma_m)$ is derived from the structural analysis, Γ_m is the basic random variable, Φ_i is considered deterministic and constant with scour depth, and load partial factors have been assumed equal to 1.0. The unit weight of masonry Γ_m is assumed normally distributed with mean value $\overline{\gamma}_m$ and coefficient of variation CoV_v . The eccentricity of loads has been considered in the verification via the slenderness and eccentricity factor Φ_i (BSI, 2013)

$$\Phi_i = 1 - 2(e_i/t) \tag{8}$$

where $e_i = 0.05t$ is the minimum eccentricity at the element top and t is the element thickness. In this study, dead loads, superimposed dead loads and pier local scour are the considered actions (HE, 2020c). To determine the thrust maximum value, Méry's method (Méry, 1840) is applied in the main plane (X-Y) of the case study bridge (Figure 2a). Méry (1840) supposed a three-hinge mechanism for the arch, with hinges located at the springing lines and crown, and the masonry material assumed linear elastic. The resulting scheme is structurally determined, the maximum thrust occurs at the springing level and e is equal to 1/6 of the arch's thickness. Therefore, the expressions for $S_a(\Gamma_m)$ was derived using equilibrium equations, and then implemented in Jupiter notebooks with Python (PSF, 2022).

Subsequently, R_c in Equation 2 and Γ_m in Equation 7 have been sampled with simple MC simulations (Schmidt et al., 2019) to estimate $R(R_c)$ and $E(\Gamma_m)$. Then, the arch probability of failure P_f has been calculated as:

$$P_f \approx n(M(x) \le 0)/N \tag{9}$$

where N is the number of conducted simulations and $n(M(x) \leq 0)$ is the number of simulations n for which $M(x) \leq 0$ according to Equation 1. A convergence assessment of the MC estimator for both R_c and Γ_m was performed in terms of CoV following procedures in Ballio and Guadagnini (2004), i.e. root mean square of sample mean/variance divided by sample mean/variance, to identify the needed number of simulations for stabilisation of CoV values. Finally, failure probability data was fitted with a lognormal fragility function by following procedures in Baker (2015):

$$P_f = \Phi \left[\ln \left(d_{s,loc} / \hat{\theta} \right) / \hat{\beta} \right] \tag{10}$$

where $d_{s.loc}$ is the pier local scour depth, $\hat{\theta}$ and $\hat{\beta}$ are the estimates of median and log standard deviation, respectively, obtained using the maximum likelihood estimation method.

2.2 Case study

The fragility assessment was carried out on a two-span masonry arch bridge in Halifax (West Yorkshire, England), which was spanning over River Calder and that collapsed in December 2015 due to flood-induced scour (Tubaldi et al., 2018). The geometry of the bridge is typical in terms of span of various UK riverine bridge portfolios (Mathews and Hardman, 2017; Stevens et al., 2020). Figure 2a depicts the geometry of the investigated bridge, including: length of 20.30m between abutment faces; out-to-out width along the transverse direction of 3.80m; the two arches are segmental in shape, assumed of one ring, with span length of 9.26m, intrados rise of 3.45m, arch thickness of 0.50m ($r_i/L = 0.37$, $t_a/L = 0.05$); the pier has a rectangular transverse section of width 1.8m and depth 3.40m; bridge total length of 33.40m.

The masonry of arches, pier, spandrel walls, and parapet has unit weight γ_m 22 kN/m^3 (Tubaldi et al., 2018), assumed as mean value $\bar{\gamma}_m = \gamma_m$, and $CoV_v = 10\%$ (Su et al., 2020), while backfill soil has unit weight of 19 kN/m^3 (Tubaldi et al., 2018) and considered deterministic.

Regarding mechanical properties: (i) for general purpose mortar M4: $\alpha = 0.7$, $\beta = 0.3$, $f_m = 4$ MPa; (ii) for group 1 calcium silicate units: K = 0.55; (iii) for red sandstone wide blocks (Wiggins et al., 2019): CF = 1, $\delta = 1.18$ for air-dry brick testing, $f_b = 10$ MPa; (iv) resulting masonry: $f_k = 4.69$ MPa, $COV_c = 15\%$ (Conde et al., 2020), $k_{00.5} = 1.6449$, $\bar{r}_c = 6.23$ MPa.

Regarding the structural scheme (Figure 2b), parapet, spandrel walls, and backfill are considered as dead loads; the three-hinged arch lies on beam-like pier and abutments; the pier lies on beam-like shallow foundation, while abutments do not have any foundation; the foundation lies on Winkler-like spring soil; the soil-foundation modelling is outside of the scope of this study, as well as considering lateral earth pressures. Given the structure's vertical symmetry, the structural analysis is limited to half of a span; a one-meter arch barrel depth (i.e. t = 1.00m) is examined.

Before performing the probabilistic assessment, the deterministic assessment identified the arch as the component at the highest risk of failure among other components. Therefore, the

arch is the main focus of the reliability analysis performed in this study and for which the fragility function is derived.

Failure probability data was derived for six different discrete levels of local scour depth, $d_{s.loc}$ = [1.20, 1.50, 2.00, 2.30, 2.49, 2.54]m, previously investigated by Tubaldi et al. (2018), and related to a not-symmetric scour hole. Scour effects on capacity and demand were considered via the empirical coefficients of Equation 6 and Equation 8, respectively, to reflect that pier local scour induces (Tubaldi et al., 2018): cracks in the arch barrel, central pier, pier-foundation interface, and eccentricity of vertical loads. Considering that the diagonal crack F_{cM} values reduce capacity the most (HE, 2020c), this case study investigates arch diagonal cracks only. Input values for F_c are: F_{CM} = 0.3 to 0.9 for diagonal cracks, while the variation of F_{cM} with scour depth is assumed linear between F_{CM} = 0.3 for $f_{s.loc}$ = 2.54m and f_{CM} = 0.9 for $f_{s.loc}$ = 120m; f_{cm} = 1.0 for width of joint = 6mm; f_{cm} = 0.8 for joints with 10% of thickness of barrel insufficiently filled; f_{cm} = 0.9 for loose joint condition; the multiplication of f_{cm} values is based on the interpretation of arch cracking patterns and damages in tension due to pier vertical displacement and rotation determined by Tubaldi et al. (2018) via three dimensional finite element analyses. For an arch barrel depth f_{cm} = 3.1m, f_{cm} = 0.05 3.1m = 0.16m, Equation 8 gives f_{cm} = 0.90 and assumed constant with scour depth.

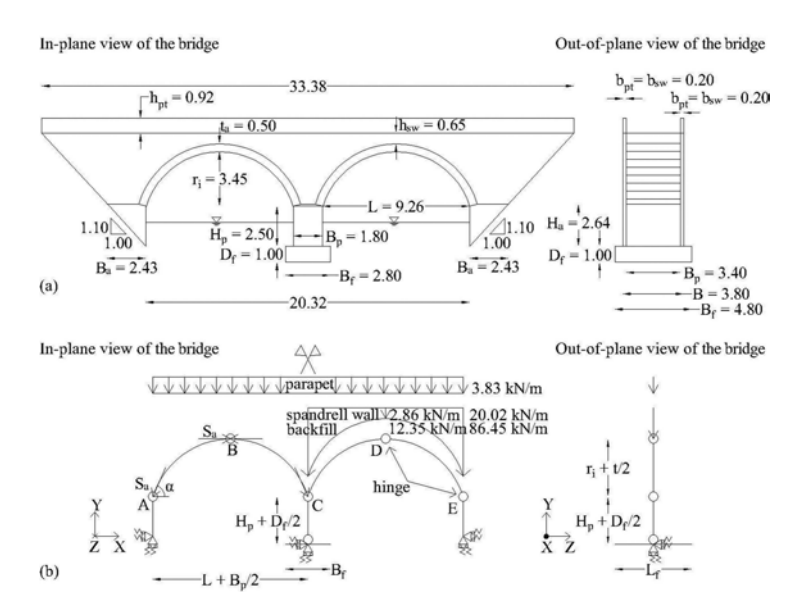


Figure 2. (a) Illustration of the case study bridge (dimensions in m); (b) model of the system bridge-river in scoured conditions.

3 RESULTS

The proposed methodology is demonstrated for the compressive failure mechanism of arches due to pier local scour for the UK case study described previously. 100.000 MC simulations were needed to obtain convergence for R_c and Γ_m in terms of CoV; the results of MC simulations are here forth referred to as "realisations". The 100.000 realisations of R_c and Γ_m were used to estimate capacity and demand according to Equation 2 and 7, respectively. Then, the obtained capacity and demand were used to estimate the limit state function (Equation 1) for the six investigated scour depths and the number of simulations for which $M(x) \leq 0$ was recorded. For instance, for $d_{s,loc} = 1.50m$, $F_c = 0.900$ and $\Phi_i = 0.90$, lead to 39.879 failures ($M(x) \leq 0$). Therefore, the first-not-null failure probability point is (1.50m, 0.3988); further points were determined by changing F_c at each investigated scour depth, while Φ_i was considered constant, followed by performing MC simulations.

The derived scour fragility function for the arch is shown in Figure 3 for a scour depth range of 1.00m to 2.6m, where 1.0m is the foundation's depth and 2.6m is just above the 2.54m collapse scour depth estimated by Tubaldi et al. (2018). Note that the minimum value considered for scour depth is 1.20m because pier displacements develop only after scour depth exceeds the foundation depth (i.e. 1.0m). From fitting the failure probability data, a median $\hat{\theta} = 1.52m$ and log standard deviation of $\hat{\beta} = 0.05$ were estimated.

The proposed approach for deriving arch scour fragility functions could be repeated for a different bridge geometry and the resulting fragility function could be used to predict the failure probability of a masonry arch, if measurements of pier scour depth is available at the bridge site. Provided the made assumptions (see Section 4), the derived fragility function shown in Figure 3 represents one of the inputs needed to determine the bridge fragility function(s) in a failure mode analysis when multiple components are considered (e.g. piers, foundation). To the authors' knowledge, the derived arch scour fragility function represents the first attempt in the literature to determine flood fragility functions of masonry arch bridges from component fragilities.

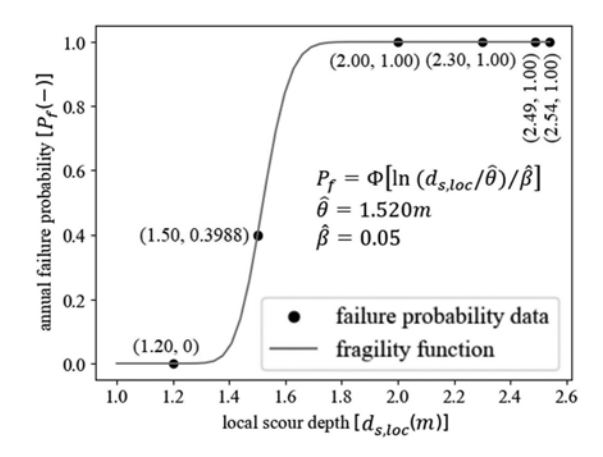


Figure 3. Derived scour fragility function for the investigated masonry arch.

4 DISCUSSION AND FUTURE RESEARCH

The proposed deriving methodology for flood fragility functions for masonry arch bridges advances the existing literature. Towards defining reliable fragility estimates, this study investigated the fragility of a masonry arch for the compressive resistance assessment, considering effects of pier local scour on arch demand and capacity; a UK case study was used to demonstrate the methodology. Results (Figure 3) showed that the investigated arch presents a median value of pier local scour depth of approximately 1.50m.

In the calculations, assumptions were made for dimensions and quality of bricks and mortar because no information was available. The effects of scour on the arch were considered via empirical coefficients (i.e. F_c , Φ_i), subjectively linked to scour depth because no relations were found. Furthermore, this study investigated a reduction of arch capacity due to diagonal cracks only, but other cracks (e.g. longitudinal) are possible (HE, 2020c). In addition, the interaction between backfill-arch-spandrel walls shall be investigated since it may affect the bridge flood response (Sarhosis et al., 2016). Failure probability data was fitted with a lognormal fragility function, which was shown to provide equal failure probabilities of other possible functions (Lallemant et al., 2015); however, more failure data shall be generated from the discretization of the expressions of condition factor F_c and eccentricity factor Φ_i as function of scour depth.

Although this work presents a fragility function for one component only (arch), it recommends to extend the methodology to the other components, to avoid underestimating the risk failure of a bridge (Nielson and DesRoches, 2007). Future work will develop scour fragility functions for compression limit state of other bridge components, such as pier, to obtain the global failure fragility

function(s). Further studies could consider additional random variables, e.g. shear strength of the mortar, to understand if there is more than one fragility function for a considered damage state; epistemic uncertainties, e.g. variability in the parameters of the used probability distribution function, shall be addressed and validated to enable implementation of fragility functions.

5 CONCLUSIONS

This study proposes a deriving methodology for scour fragility functions of masonry arch bridges able to account for failure modes of significant bridge components, which represents a novelty in the existing literature. Using a UK case study, a fragility function for the arch of a masonry bridge subjected to pier local scour was derived via simple MC simulations and analytical design expressions as an example. Future research opportunities include: (a) applying the proposed methodology to other bridge components; (b) investigating the relations scour depth-masonry capacity and demand; (c) investigating effects of various epistemic uncertainties; (d) validating the developed fragility functions.

DATA STATEMENT

Data and codes underpinning this paper are available upon request to the main author.

ACKNOWLEDGMENTS

Giuseppe Degan Di Dieco and Maria Pregnolato acknowledge the Engineering and Physical Sciences Research Council (EPSRC) (Scholarship 2444849; Fellowship EP/R00742X/2), The Alan Turing Institute (ATI) (2021/22 Enrichment Scheme), Dr Mark Hobbs from The ATI for his supervision, and Sophia Nunn for proofreading.

REFERENCES

- Ang, A. H. S. & Tang, W. H. 1975. Probability Concepts in Engineering Planning and Design, Vol. 1 -Basic Principles. New York: John Wiley & Sons.
- Argyroudis, S. A. & Mitoulis, S. A. 2021. Vulnerability of bridges to individual and multiple hazards-floods and earthquakes. *Reliability Engineering & System Safety* 210.
- Baker, J. W. 2015. Efficient analytical fragility function fitting using dynamic structural analysis. *Earth-quake Spectra* 31(1): 579–599.
- Ballio, F. & Guadagnini, A. 2004. Convergence assessment of numerical Monte Carlo simulations in groundwater hydrology. *Water Resources Research* 40(4).
- BSI. 2013. BS EN 1996-1-1:2005+A1:2012. General rules for reinforced and unreinforced masonry structures. London: British Standards Institute.
- BSI. 2015. BS EN 772-1:2011+A1:2015. Methods of test for masonry units Part 1: Determination of compressive strength. London: British Standards Institute.
- Burns, P. O., Barbosa, A. R., Olsen, M. J. & Wang, H. 2021. Multihazard Damage and Loss Assessment of Bridges in a Highway Network Subjected to Earthquake and Tsunami Hazards. *Natural Hazards Review* 22(2).
 Como, M. 2013. *Statics of Historic Masonry Constructions*. New York: Springer.
- Conde, B., Matos, J. C., Oliveira, D. V. & Riveiro, B. 2020. Probabilistic-based structural assessment of a historic stone arch bridge. *Structure and Infrastructure Engineering*: 1–13.
- Degan Di Dieco, G., Barbosa, A. R. & Pregnolato, M. 2022. A taxonomy of riverine roadway bridges at risk of flooding: towards bridge classes and damage models. *Proceedings of the Institution of Civil Engineers Bridge Engineering*: 1–15.
- Eidsvig, U., Santamaría, M., Galvão, N., Tanasic, N., Piciullo, L., Hajdin, R., Nadim, F., Sousa, H. S. & Matos, J. 2021. Risk Assessment of Terrestrial Transportation Infrastructures Exposed to Extreme Events. *Infrastructures* 6(11).
- Fang, D. L., Napolitano, R. K., Michiels, T. L. & Adriaenssens, S. M. 2019. Assessing the stability of unreinforced masonry arches and vaults: a comparison of analytical and numerical strategies. *Inter*national Journal of Architectural Heritage 13(5): 648–662.
- Galasso, C., Pregnolato, M. & Parisi, F. 2021. A model taxonomy for flood fragility and vulnerability assessment of buildings. *International Journal of Disaster Risk Reduction* 53.

- George, J. & Menon, A. 2021. A mechanism-based assessment framework for masonry arch bridges under scour-induced support rotation. *Advances in Structural Engineering* 24(12): 2622–2636.
- Gidaris, I., Padgett, J. E., Barbosa, A. R., Chen, S., Cox, D., Webb, B. & Cerato, A. 2017. Multiple-Hazard Fragility and Restoration Models of Highway Bridges for Regional Risk and Resilience Assessment in the United States: State-of-the-Art Review. *Journal of Structural Engineering* 143(3): 04016188.
- HE. 2020a. CD 356: Design of highway structures for hydraulic action Revision 1. London: Highways England.
- HE. 2020b. CD 376: Unreinforced masonry arch bridges Revision 0. London: Highways England.
- HE. 2020c. CS 454: Assessment of highway bridges and structures Revision 1. London: Highways England. Lallemant, D., Kiremidjian, A. & Burton, H. 2015. Statistical procedures for developing earthquake damage fragility curves. Earthquake Engineering & Structural Dynamics 44(9): 1373–1389.
- Lamb, R., Garside, P., Pant, R. & Hall, J. W. 2019. A Probabilistic Model of the Economic Risk to Britain's Railway Network from Bridge Scour During Floods. Risk Analysis 39(11): 2457–2478.
- Li, X., Cooper, J. R. & Plater, A. J. 2021. Quantifying erosion hazards and economic damage to critical infrastructure in river catchments: Impact of a warming climate. Climate Risk Management 32: 100287.
- Mangalathu, S., Soleimani, F. & Jeon, J.-S. 2017. Bridge classes for regional seismic risk assessment: Improving HAZUS models. *Engineering Structures* 148: 755–766.
- Maroni, A., Tubaldi, E., Val, D., McDonald, H., Lothian, S., Riches, O., Zonta, D. & Huang, H. 2020.
 A Bayesian network-based decision framework for managing bridge scour risk. Sensors and Smart Structures Technologies for Civil, Mechanical, and Aerospace Systems 2020.
- Mathews, R. & Hardman, M. 2017. Lessons learnt from the December 2015 flood event in Cumbria, UK. *Proceedings of the Institution of Civil Engineers Forensic Engineering* 170(4): 165–178.
- Melchers, R. E. & Beck, A. T. 2018. Structural Reliability Analysis and Prediction. Hoboken: Wiley.
- Mendoza Cabanzo, C., Santamaría, M., Sousa, H. S. & Matos, J. C. 2022. In-Plane Fragility and Parametric Analyses of Masonry Arch Bridges Exposed to Flood Hazard Using Surrogate Modeling Techniques. *Applied Sciences* 12(4).
- Méry, E. 1840. Sur l'équilibre des voûtes en berceau. *Annales des Ponts et Chaussées* 1er Sèrie(1er Semestre). Minnucci, L., Scozzese, F., Carbonari, S., Gara, F. & Dall'Asta, A. 2022. Innovative Fragility-Based Method for Failure Mechanisms and Damage Extension Analysis of Bridges. *Infrastructures* 7(9).
- Morton, J. 2012. Designers' Guide to Eurocode 6: Design of Masonry Structures. London: ICE Publishing.
- Nielson, B. G. & DesRoches, R. 2007. Seismic fragility methodology for highway bridges using a component level approach. *Earthquake Engineering & Structural Dynamics* 36(6): 823–839.
- PSF. 2022. Python 3.11.1 documentation. The Internet: Python Software Foundation.
- Ren, L., He, S., Yuan, H. & Zhu, Z. 2019. Seismic Fragility Analysis of Bridge System Based on Fuzzy Failure Criteria. *Advances in Civil Engineering*: 1–13.
- Sarhosis, V., De Santis, S. & de Felice, G. 2016. A review of experimental investigations and assessment methods for masonry arch bridges. *Structure and Infrastructure Engineering* 12(11): 1439–1464.
- Sasidharan, M., Parlikad, A. K. & Schooling, J. 2021. Risk-informed asset management to tackle scouring on bridges across transport networks. Structure and Infrastructure Engineering: 1–17.
- Schaap, H. S. & Caner, A. 2021. Bridge collapses in Turkey: causes and remedies. Structure and Infrastructure Engineering: 1–16.
- Schmidt, R., Voigt, M., Pisaroni, M., Nobile, F., Leyland, P., Pons-Prats, J. & Bugeda, G. 2019. General Introduction to Monte Carlo and Multi-level Monte Carlo Methods. Uncertainty Management for Robust Industrial Design in Aeronautics. Springer International Publishing.
- Shinozuka, M., Feng, M. Q., Lee, J. & Naganuma, T. 2000. Statistical Analysis of Fragility Curves. *Journal of Engineering Mechanics* 126(12).
- Solan, B., Ettema, R., Ryan, D. & Hamill, G. A. 2020. Scour Concerns for Short-Span Masonry Arch Bridges. *Journal of Hydraulic Engineering* 146(2).
- Stevens, N. A., Lydon, M., Marshall, A. H. & Taylor, S. 2020. Identification of Bridge Key Performance Indicators Using Survival Analysis for Future Network-Wide Structural Health Monitoring. Sensors (Basel) 20(23).
- Su, L., Li, X.-l. & Jiang, Y.-p. 2020. Comparison of methodologies for seismic fragility analysis of unreinforced masonry buildings considering epistemic uncertainty. *Engineering Structures* 205.
- Swiss Re 2021. Global insured catastrophe losses rise to USD 112 billion in 2021, the fourth highest on record. Swiss Re Press Releases.
- Tubaldi, E., Macorini, L. & Izzuddin, B. A. 2018. Three-dimensional mesoscale modelling of multi-span masonry arch bridges subjected to scour. *Engineering Structures* 165: 486–500.
- Wen, Y. K. & Ellingwood, B. R. 2005. The Role of Fragility Assessment in Consequence-Based Engineering. *Earthquake Spectra* 21(3): 861–877.
- Wiggins, D., Mudd, K. & Healey, M. 2019. Rehabilitation of Brougham Castle Bridge, UK. *Proceedings of the Institution of Civil Engineers Engineering History and Heritage* 172(1): 7–18.